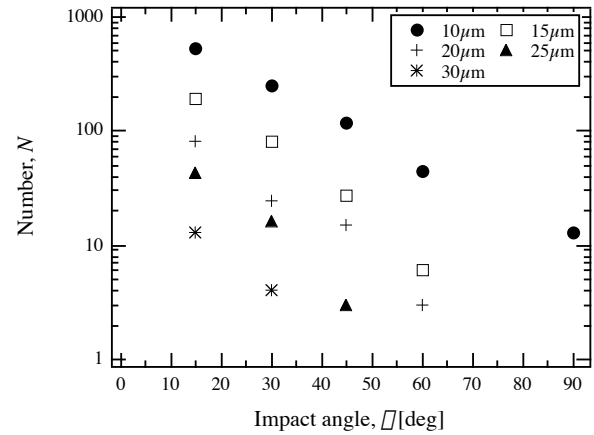


**MEASUREMENTS OF EJECTA VELOCITY DISTRIBUTION FROM REGOLITH TARGETS IN OBLIQUE IMPACTS.** S. Yamamoto<sup>1</sup>, T. Kadono<sup>2</sup>, S. Sugita<sup>3</sup>, and T. Matsui<sup>1</sup>, <sup>1</sup>Graduate School of Frontier Sciences, University of Tokyo, Tokyo 113-0033, Japan ([yamachan@gfd-dennou.org](mailto:yamachan@gfd-dennou.org)), <sup>2</sup>IFREE, JAMSTEC, Kanagawa 273-0061, Japan, <sup>3</sup>Department of Earth and Planetary Sciences, University of Tokyo, Tokyo 113-0033, Japan

**Introduction:** The velocity distribution of impact ejecta from regolith-like target has been investigated in laboratory for nearly three decades. For the case of vertical impact, the ejecta velocity distribution is determined experimentally and given by a power-law with an exponent of  $-1.22$  [1]. There is an upper limit to the ejecta velocity (Hartmann cutoff velocity) that depends on impact velocity [2]. On the contrary, for the case of oblique impacts, it was reported that there exists a separate group of high-velocity ejecta component above the Hartmann cutoff velocity [3][4]. However, there are few studies concerning the velocity distribution of the high-velocity ejecta component for oblique impacts. More data and further investigation are obviously required to quantify the ejecta velocity distributions from regolith targets for various impact angles. Therefore we performed impact experiments on sand targets for various impact angles, in order to measure the ejecta velocity distribution of the high-velocity component above the Hartmann cutoff velocity.

**Experiments:** Regolith targets were simulated by soda-lime glass powders with density of  $2.5 \text{ g cm}^{-3}$ . The mean diameter of the glass spheres was  $229 \mu\text{m}$ . Copper projectiles with mass of  $0.27 \text{ g}$  were accelerated to  $226$  to  $260 \text{ ms}^{-1}$  by an electromagnetic gun. The electromagnetic gun can be tilted at various angles ( $\varphi=15, 30, 45, 60$ , and  $90^\circ$  to the target). The ejecta were detected by secondary targets (thin aluminum foil set around the glass powders). The ejecta with sufficient velocities can penetrate the secondary targets, and then leave holes on the foil. The thicknesses  $f$  of the foil were  $10, 15, 20, 25, 30$ , and  $40 \mu\text{m}$ . By using a transmission microscope, the number of holes penetrated by ejecta was measured. Figure 1 shows that the total number  $N$  of holes on the aluminum foil for each shot. The result clearly shows that  $N$  increases with decrease in  $\varphi$ . It is noted that there is the critical thickness of the foil that ejecta can penetrate. For example, no ejecta can penetrate the aluminum foil with  $f=25 \mu\text{m}$  or  $f=30 \mu\text{m}$  at  $\varphi=60^\circ$ . There was no holes on the aluminum foil with  $f=40 \mu\text{m}$ .



**Figure 1:** Number of holes on the aluminum foil with various thicknesses.

**Velocity distribution:** The ejecta velocity distribution was obtained as follows. From the analysis of the foil, the spatial distributions of the ejecta that can penetrate the foil were derived in a way similar to the previous studies [3][4]. Integrating the resulting spatial distribution, we derived the total volume  $V$  of ejecta that can penetrate the aluminum foil for each experiment. In order to obtain the velocity distribution, it is necessary to know the lower-limit velocity of particles needed to penetrate the aluminum foil. Based on the results of the experiments by Yamamoto [3], the lower-limit velocities for the foil with  $f=10, 15, 20, 25$ , and  $30 \mu\text{m}$  are estimated to be  $85, 104, 120, 134$ , and  $146 \text{ ms}^{-1}$ , respectively. The velocity region measured here is above the Hartmann cutoff velocity, which is estimated to be about  $46$  to  $67 \text{ ms}^{-1}$  for our experimental condition. Therefore, the ejecta detected by the foil used here correspond to the group of the high-velocity ejecta component.

**Results:** The ejecta volume  $V$  normalized by  $R^3$  ( $R$  is the crater radius for each shot) is plotted against ejecta velocity in Figure 2. It is clear that the normalized ejecta volume ( $V/R^3$ ) increases with decrease in impact angle. The results at  $\varphi=15^\circ$  are about two orders of magnitude greater than those at  $\varphi=90^\circ$  (vertical impact) or  $\varphi=60^\circ$ .

## Ejecta velocity distribution: S. Yamamoto et al.

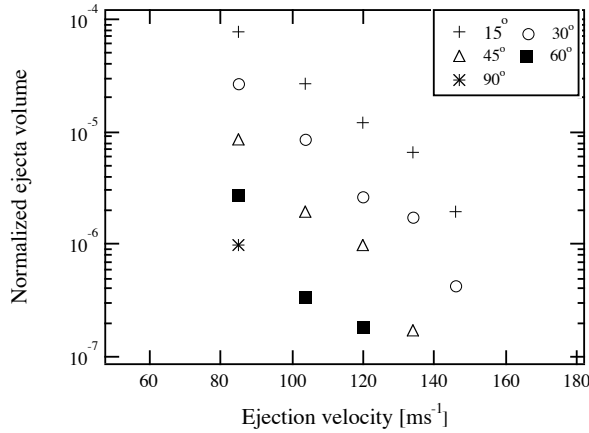


**Figure 2:** The normalized ejecta volumes with ejection velocities greater than a given value are plotted against the ejection velocity for various impact angle  $\varphi$ .

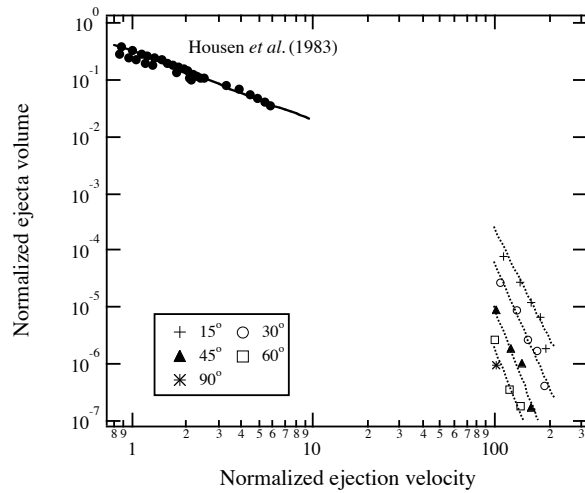


**Figure 3:** The normalized ejecta volumes with ejection velocities greater than a given value are plotted against the normalized ejection velocity. For comparison, a scaling formula (solid line) based on the data (filled circles) for ejecta with lower ejection velocity (Housen *et al.* [1]) is also plotted. The dotted lines represent the least-squares fit to the data for each impact angle.

We can compare our results with other experimental data on lower velocity ejecta below the Hartmann cutoff velocity by using the scaling formula [1]. In Figure 3 the normalized ejecta volumes are plotted against the ejection velocity normalized by  $(gR)^{0.5}$ . Assuming the power-law distribution, the slopes of  $V/R^3$  of our data at 15, 30, 45, and 60° are estimated to be -6.4, -7.3, -8.2, and -8.1 (dotted line), respectively. These slopes are steeper than that of -1.22 (solid line) for the Housen *et al.* data [1].

We can see in figure 2 that there are the upper-limit

velocities  $v_1$  at which no holes were observed on the aluminum foil. Then the upper-limit velocities are plotted against  $\varphi$  in Figure 4. The upper and lower values of each error bar are  $v_1$  and  $v_2$ , respectively.  $v_2$  is another upper limit velocity, which is defined by the thickest foil that ejecta can penetrate. The actual upper-limit velocity must lie between  $v_1$  and  $v_2$ . We can see a trend in Figure 4 that the upper-limit velocity of the ejecta increases with decrease in  $\varphi$ . From the experiment using high-speed camera, the highest expanding velocity of the ejecta curtain at  $\varphi=15^\circ$  was measured to be about 2.5 times faster than that for the vertical impacts [3]. It is therefore suggested that the velocity distribution of the high-velocity ejecta component would shift to right (higher velocity) with decrease in  $\varphi$  (see Figure 3). The upper-limit velocity might be related to the Hartmann cutoff velocity. If so, the Hartmann cutoff velocity would depend on the impact angles as well as the impact velocities.

**Summary:** We can separate impact ejecta into two groups; one is the ejecta with lower ejection velocity and the other is the ejecta with higher ejection velocity (higher than the Hartmann cutoff velocity). Below the Hartmann cutoff velocity, the ejecta velocity distribution has the power-law with an exponent of about -1.2. Above the cutoff velocity, the slopes of the high-velocity ejecta become to be very steep. The velocity distribution of the high-velocity ejecta component depends on the impact angle. It is a future problem to understand how we scale these observations to a simple scaling formula.

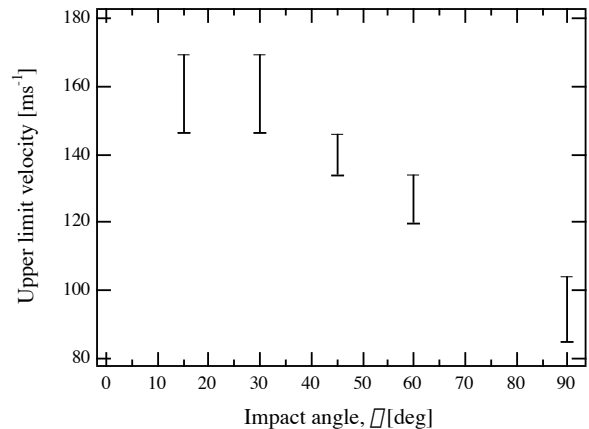


**Figure 4:** Upper limit velocities are plotted against the impact angle  $\varphi$ .

**References:** [1] Housen K.R. *et al.*, (1983) *JGR*, 88, 2485-2499. [2] Hartmann W.K., (1985) *Icarus*, 63, 69-98. [3] Yamamoto S., (2002) *Icarus*, 158, 87-97. [4] Yamamoto S. & Nakamura A.M., (1997) *Icarus*, 128, 160-170.